

Progress on NNLO CTEQ PDFs and Neutral-current DIS at NNLO in the general-mass scheme

Pavel Nadolsky

Southern Methodist University
Dallas, TX, U.S.A.

in collaboration with
M. Guzzi, F. Olness,
J. Huston, H.-L. Lai, Z. Li, J. Pumplin, C.-P. Yuan
September 27, 2011

Recent work on...

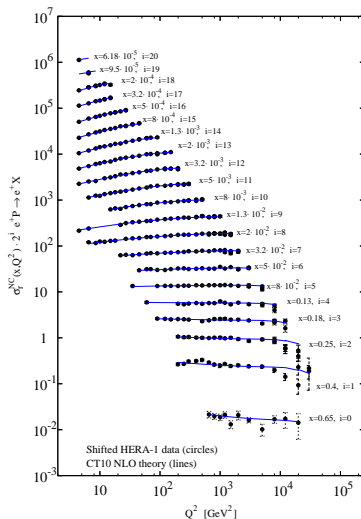
- CT10.1 NLO and NNLO PDF fits
- Heavy-quark contributions to neutral-current DIS at NNLO

In backup slides:

- extended discussion of the Tevatron Run-2 W asymmetry data – the CT10W fit to Tevatron Run-2 data
- fits to Tevatron jet cross sections
- search for deviations from NLO DGLAP evolution in the small- x HERA data (not observed)
- benchmark comparisons of NNLO PDF fits

CT10 parton distribution functions (PRD82, 074024 (2010))

- General-purpose NLO PDFs
- Adequate for the majority of PQCD applications
- includes combined HERA-1 DIS, Tevatron Run-2 inclusive jet, Z rapidity data
- detailed analysis of the Tevatron Run-2 W asymmetry (A_ℓ) data
 - ▶ CT10 and CT10W sets, with different treatment of A_ℓ



CT10 parton distribution functions (PRD82, 074024 (2010))

- 53 CT10/CT10W eigenvector sets for $\alpha_s(M_Z) = 0.118$

- ▶ 4 CT10AS/CT10WAS PDFs for $\alpha_s(M_Z) = 0.116 - 0.120$

- ◇ The correlated PDF+ α_s uncertainty on an observable X is computed by

$$\Delta X_{PDF+\alpha_s} = \sqrt{\Delta X_{PDF, CT10}^2 + \Delta X_{\alpha_s, CT10AS}^2},$$

as explained in PRD 82,054021 (2010)

- ▶ CT10/CT10W PDFs with 3 and 4 active flavors
- In the LHADPF library and at <http://hep.pa.msu.edu/cteq/public/index.html>

CT10.1 global PDF analysis

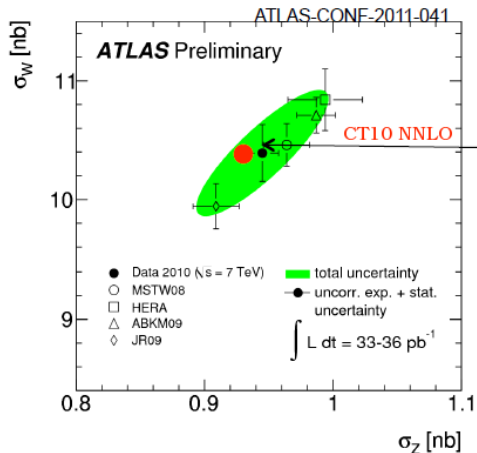
In the pre-publication stage

- CT10.1 NLO set: extension of the CT10W analysis, with alternative treatment of some data sets
 - ▶ D0 Run-2 electron charge asymmetry (A_ℓ) – include only most inclusive $p_{T\ell}$ bins (theoretically clean)
 - ▶ Alternative fits with reduced weight on experiments with larger theory uncertainties: $F_2^{p,d}$ from BCDMS & NMC, Tevatron Run-1 incl. jets
- CT10.1 NNLO PDFs
 - ▶ Validation of heavy-quark S-ACOT scheme at $O(\alpha_s^2)$
 - ▶ $\alpha_s(M_Z) = 0.118$, $m_c^{pole} = 1.3$ GeV, $m_b^{pole} = 4.75$ GeV (same as in CT10.1 NLO PDFs)

CT10.1 NNLO fit

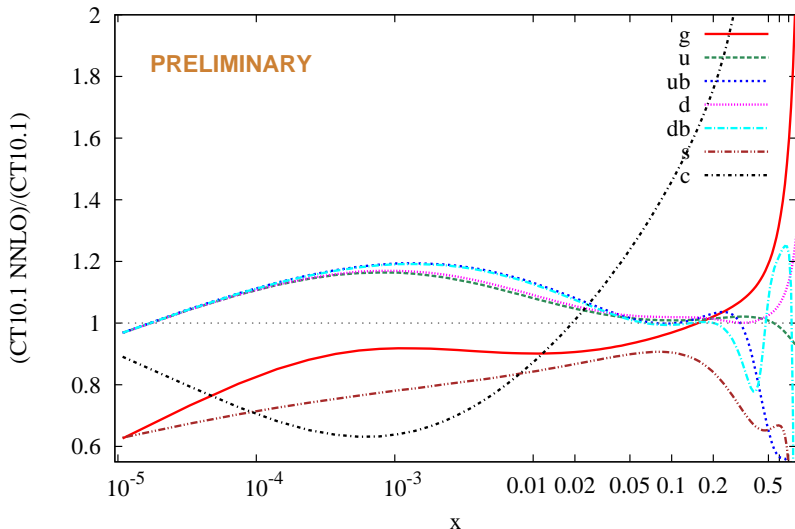
- Candidate central fits are available (cf. the next slide)
- In progress: studies of parametrization dependence, PDF errors
- The same $\chi^2/N_{pt} \approx 3100/2765 \approx 1.12$ at NLO and NNLO
- Differences between NLO and NNLO sets are comparable to such differences in ABM & MSTW NNLO PDF sets
- Reduced gluon at $x \rightarrow 0$; increased light quarks at $x \approx 10^{-3}$; lower strangeness

CT10.1 NNLO predictions for LHC W and Z cross sections



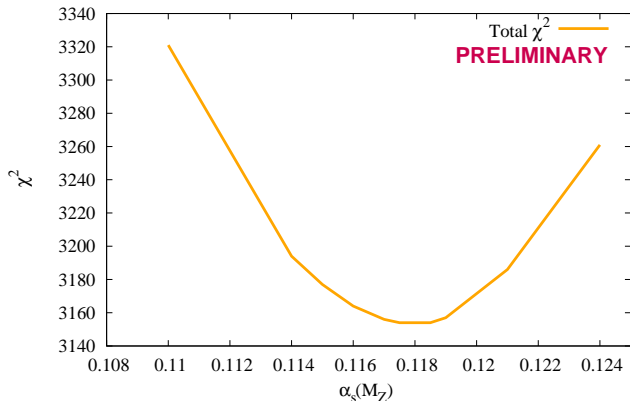
Candidate NNLO fit (compared to CT10.1 NLO)

Ratios of central CT10.1 PDFs $\mu = 2$ GeV



Dependence on α_s in the CT10.1 fit

CT10.2 NNLO candidate



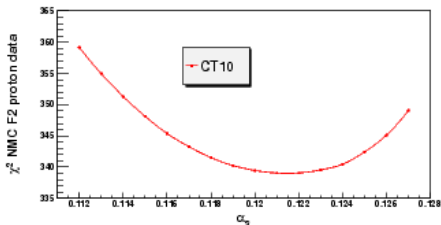
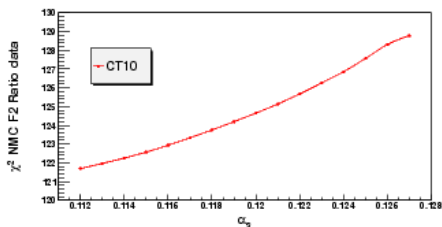
α_s decreases slightly at NNLO, has about the same PDF uncertainty as at NLO

■ NLO: $\alpha_s(M_Z) = 0.11964 \pm 0.0064$ at 90% c.l.

■ NNLO: $\alpha_s(M_Z) = 0.118 \pm 0.005$

CT10AS fit: NMC F_2^d/F_2^p and F_2^p data vs. α_s

Total χ^2 vs. $\alpha_s(M_Z)$ in the CT10AS series



■ We did not find a significant effect of the NMC F_2^d/F_2^p data on α_s , even though a smaller value is mildly preferred. $\chi^2(F_2^d/F_2^p) \approx N_{points} = 123$.

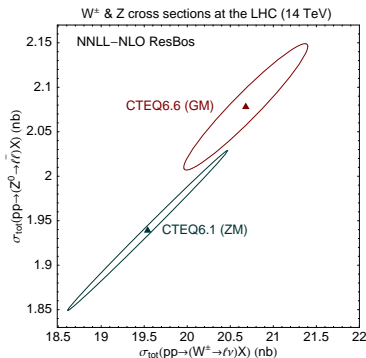
■ NMC F_2^p data prefer a larger α_s , but χ^2 is larger than $N_{points} = 201$.

■ Replacing F_2^p by the NMC reduced cross section does not significantly change the best-fit value of α_s and its error.

Massive parton contributions to DIS cross sections

Among numerous influences on the PDFs, treatment of massive quarks stands out because of its significance for precise QCD predictions for the LHC (*Tung et al., hep-ph/0611254*)

- Quark mass effects in DIS are comparable to NNLO terms
- Several heavy-quark schemes are available (*FFN, ACOT, BMSN, CSN, FONLL, TR'...*)
- Despite extensive recent work, some confusions about basic questions persist, e.g., about the universality of heavy-quark PDFs



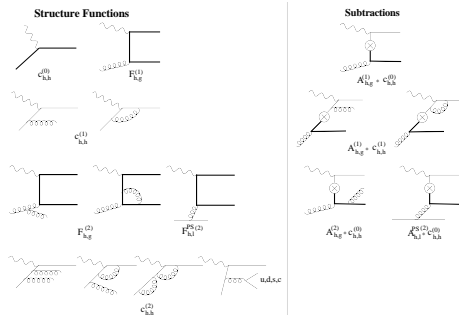
Tung et al., hep-ph/0611254; Thorne, hep-ph/0601245; Tung, Thorne, arXiv:0809.0714; PN., Tung, arXiv:0903.2667; Forte, Laenen, Nason, arXiv:1001.2312; J. Rojo et al., arXiv:1003.1241; Alekhin, Moch, arXiv:1011.5790;...

Neutral-current DIS in S-ACOT- χ scheme at NNLO

M. Guzzi, P.N., H.-L. Lai, C.-P. Yuan, arXiv:1108.5112 (hep-ph)

Objectives

- elucidate fundamental principles that a viable GM scheme must satisfy
- modify the QCD factorization theorem for DIS with massive quarks (*Collins, 1998*) to satisfy momentum conservation in all heavy-quark scattering channels
- provide algorithmic implementation of NNLO massive contributions

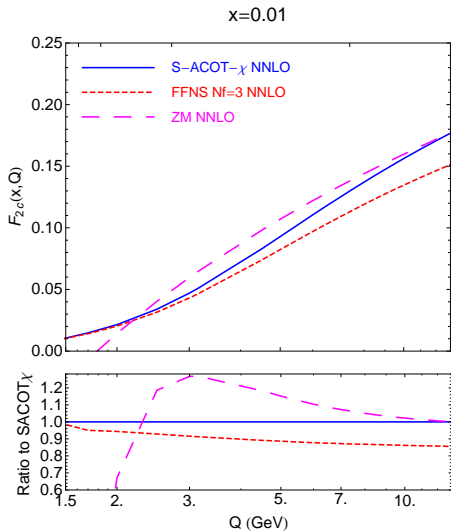


NNLO scattering contributions

Details of the NNLO computation

- NNLO evolution for α_s and PDFs (HOPPET)
 - ▶ matching coefficients relating the PDFs in N_f and N_{f+1} schemes (*Smith, van Neerven, et al.*)
- NNLO Wilson coefficient functions for $F_2(x, Q)$, $F_L(x, Q)$
- Pole quark masses or \overline{MS} quark masses as an input
- CT10.1: pole masses $m_c = 1.3$ GeV, $m_b = 4.75$ GeV (as in CT10)

S-ACOT- χ scheme: merging FFN and ZM

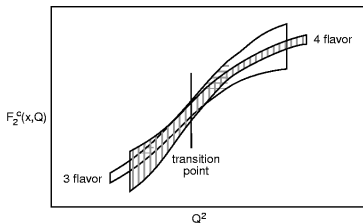


ACOT reduces
to FFNS at $Q \approx m_c$
and to ZM at $Q \gg m_c$

Les Houches toy PDFs, evolved
at NNLO with threshold
matching terms

Cancellations between
subtractions and other terms at
 $Q \approx m_c$ and $Q \gg m_c$; details in
backup slides

General-Mass Variable Flavor Number schemes



(Aivasis, Collins, Olness, Tung; Buza et al.; Cacciari, Greco, Nason; Chuvakin et al.; Kniehl et al.; Thorne, Roberts; Forte, Laenen, Nason; ...)

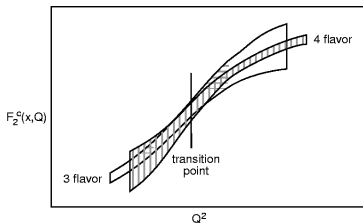
For the ACOT GM scheme, factorization of DIS cross sections is proved to all orders of α_s (Collins, 1998)

Theorem

$$F_2(x, Q, m_c) = \sigma_0 \sum_{a=g, q, \bar{q}} \int \frac{d\xi}{\xi} C_a \left(\frac{x}{\xi}, \frac{Q}{\mu_F}, \frac{m_c}{Q} \right) f_{a/p}(\xi, \frac{\mu_F}{m_c}) + \mathcal{O} \left(\frac{\Lambda_{QCD}}{Q} \right)$$

- C_a is a Wilson coefficient with an incoming parton $a = g, \bar{u}, \dots, \bar{c}$
- $f_{a/p}$ is a PDF for N_f flavors
- $N_f = 3$ for $\mu < \mu_{switch}^{(4)} \approx m_c$; $N_f = 4$ for $\mu \geq \mu_{switch}^{(4)}$
- $\lim_{Q \rightarrow \infty} C_a$ exists; no terms $\mathcal{O}(m_c/Q)$ in the remainder

General-Mass Variable Flavor Number schemes



(Aivasis, Collins, Olness, Tung; Buza et al.; Cacciari, Greco, Nason;
Chuvakin et al.; Kniehl et al.; Thorne, Roberts; Forte, Laenen, Nason; ...)

For the ACOT GM scheme,
factorization of DIS cross sections is
proved to all orders of α_s (Collins, 1998)

Schemes of the ACOT type do not use...

- PDFs for several N_f values in the same μ range
- smoothness conditions/damping factors at $Q \rightarrow m_c$
- constant terms from higher orders in α_s to ensure continuity at the threshold

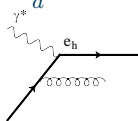
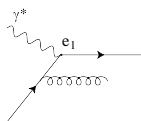
Components of inclusive $F_{2,L}(x, Q)$

Structure of S-ACOT- χ NNLO expressions is reminiscent of the ZM scheme (e.g., in Moch, Vermaseren, Vogt, 2005)

Components of inclusive $F_{2,L}(x, Q^2)$ are classified according to the quark couplings to the photon

$$F = \sum_{l=1}^{N_l} F_l + F_h \quad (1)$$

$$F_l = e_l^2 \sum_a [C_{l,a} \otimes f_{a/p}] (x, Q), \quad F_h = e_h^2 \sum_a [C_{h,a} \otimes f_{a/p}] (x, Q). \quad (2)$$



At

$\mathcal{O}(\alpha_s^2)$:

$$F_h^{(2)} = e_h^2 \left\{ c_{h,h}^{NS,(2)} \otimes (f_{h/p} + f_{\bar{h}/p}) + C_{h,l}^{(2)} \otimes \Sigma + C_{h,g}^{(2)} \otimes f_{g/p} \right\}$$

$$F_l^{(2)} = e_l^2 \left\{ C_{l,l}^{NS,(2)} \otimes (f_{l/p} + f_{\bar{l}/p}) + c^{PS,(2)} \otimes \Sigma + c_{l,g}^{(2)} \otimes f_{g/p} \right\}. \quad (3)$$

Components of inclusive $F_{2,L}(x, Q)$

- Lower case $c_{a,b}^{(2)}, \hat{f}_{a,b}^{(k)} \rightarrow$ ZM expressions
Zijlstra and Van Neerven PLB272 (1991), NPB383 (1992)
S. Moch, J.A.M. Vermaseren and A. Vogt, NPB724 (2005)
- Upper case $C_{a,b}^{(2)}, F_{a,b}^{(k)}, A_{a,b}^{(k)} \rightarrow$ coeff. functions, structure functions and subtractions with $m_c \neq 0$,
Buza *et al.*, NPB 472 (1996); EPJC 1 (1998);
Riemersma, *et al.* PLB 347 (1995); Laenen *et al.* NPB392 (1993)
- All building blocks are available from literature

Components of inclusive $F_{2,L}(x, Q)$

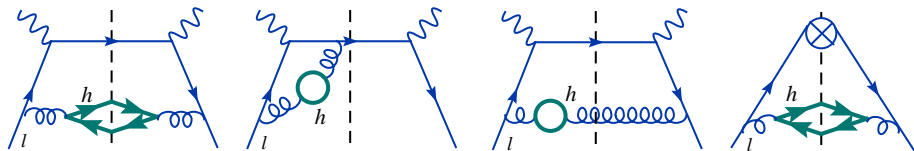
The separation into F_l and F_h (according to the quark's electric charge e_i^2) is valid at all Q

The “light-quark” F_l contains some subgraphs with heavy-quark lines, denoted by “ $G_{l,l,heavy}$ ”.

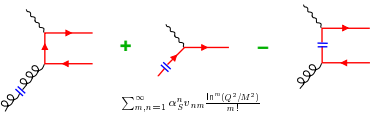
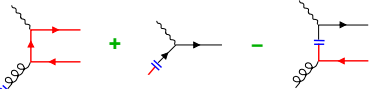
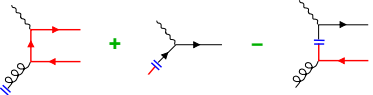
The “heavy-quark” $F_h \neq F_2^c$:

$$F_2^c = F_h + (G_{l,l,heavy})_{real},$$

where $G_{i,j} = C_{i,j}^{(2)}$, $F_{i,j}^{(2)}$, and $A_{i,j}^{(2)}$



Three versions of the ACOT scheme

Scheme	Lowest-order graphs	Variables in H_c
Full ACOT <i>Aivasis et. al., hep-ph/9312319</i> <i>Proof in Collins, hep-ph/9806259</i>	 $\sum_{m,n=1}^{\infty} \alpha_s^n v_{nm} \frac{\ln^m(Q^2/M^2)}{m!}$	$m_c \neq 0$ $\zeta = \frac{\beta}{2} \left(1 + \sqrt{1 + \frac{4m_c^2}{Q^2}} \right)$
Simplified ACOT <i>Proof in Collins, hep-ph/9806259;</i> <i>Kramer, Olness, Soper, hep-ph/0003035</i>		$m_c = 0$ $\zeta = x$
S-ACOT-χ <i>Tung, Kretzer, Schmidt, hep-ph/0110247;</i> <i>proof in Guzzi et al., arXiv:1108.5112</i>		$m_c = 0$ $\zeta = x \left(1 + \frac{4m_c^2}{Q^2} \right) \equiv \chi$

■ H_a with incoming light partons are unambiguous

■ H_c with incoming c quarks differ by terms of order $(m_c^2/Q^2)^p, p > 0$

The NLO analytic result

Which would you prefer to calculate?

ACOT

$$\begin{aligned}
 \hat{\sigma}_2^{(V,0)}(\delta_1) &= \frac{8}{\Delta^2} \left\{ -\Delta^2(S_1\Sigma_{1+} - 2m_1m_0S_1)I_e + 2m_1m_0S_1 \left(\frac{1}{\delta_1} [\Delta^2 + 4m_1^2\Sigma_{1-}] \right. \right. \\
 &+ 2\Sigma_{1-} - \Sigma_{1+} + \frac{\Sigma_{1+} + \delta_1}{2} + \frac{\delta_1 + m_1^2}{\Delta\delta_1} [\Delta^2 + 2\Sigma_{1-}\Sigma_{1+} + (m_1^2 + Q^2)\delta_1] I_e \left. \right\} \\
 &+ S_1 \left(\frac{-m_1^2\Sigma_{1+}}{(\delta_1 + m_1^2)\delta_1} (\Delta^2 + 4m_1^2\Sigma_{1-}) - \frac{1}{4(\delta_1 + m_1^2)} [3\Sigma_{1+}^2\Sigma_{1-} + 4m_1^2\Sigma_{1+}\Sigma_{1-} \right. \\
 &- \Sigma_{1-}\Sigma_{1+} - m_1^2\Sigma_{1+}] + \delta_1[-7\Sigma_{1+}\Sigma_{1-} + 18\Delta^2 - 4m_1^2(Q^2 - 4m_1^2 + 7m_1^2)] \\
 &+ 3\delta_1^2[\Sigma_{1-} - 2m_1^2] - \delta_1^2 \left. \right) + \frac{\delta_1 + m_1^2}{2\Delta^2} \left[\frac{-2}{\delta_1} \Sigma_{1+} (\Delta^2 + 2\Sigma_{1-}\Sigma_{1+}) \right. \\
 &+ (4m_1^2m_1^2 - 7\Sigma_{1-}\Sigma_{1+}) - \delta_1\Sigma_{1-}\delta_1 - \delta_1^2 \left. \right] I_e \left. \right\} \\
 \hat{\sigma}_2^{(A,0)}(\delta_1) &= \frac{16}{\Delta^2} \left\{ -2\Delta^4 S_1 I_e + 2m_1m_0S_1 \left(\frac{\delta_1 + m_1^2}{\Delta} (\Delta^2 - 6m_1^2Q^2) I_e \right. \right. \\
 &- \frac{\Delta^2(\delta_1 + \Sigma_{1+})}{2(\delta_1 + m_1^2)} + (2\Delta^2 - 3Q^2)(\delta_1 + \Sigma_{1+}) \left. \right) + S_1 \left(-2(\Delta^2 - 6m_1^2Q^2)(\delta_1 + m_1^2) \right. \\
 &- 2(m_1^2 + m_1^2)\delta_1 - 9m_1^2Q^2 - \Delta^2(2\Sigma_{1+} - m_1^2) + 2\delta_1(2\Delta^2 + (m_1^2 - 5m_1^2)\Sigma_{1-}) \\
 &+ \frac{(\Delta^2 - 6Q^2)(m_1^2 + \delta_1)\Sigma_{1+}(\delta_1 + \Sigma_{1+})}{2(\delta_1 + m_1^2)} - \frac{2\Delta^2}{\delta_1} (\Delta^2 + 2\Sigma_{1+}\delta_1)\Sigma_{1-} \\
 &+ \frac{(\delta_1 + m_1^2)}{\Delta^2} \left[\frac{-2}{\delta_1} \Delta^2 (\Delta^2 + 2\Sigma_{1-}\Sigma_{1+}) - 2\delta_1(\Delta^2 - 6m_1^2Q^2) \right. \\
 &- (\Delta^2 - 18m_1^2Q^2)\Sigma_{1-} - 2\Delta^2(\Sigma_{1+} + 2\Sigma_{1-}) \left. \right] I_e \left. \right\} \\
 \hat{\sigma}_2^{(R,0)}(\delta_1) &= \frac{16}{\Delta^2} \left\{ -2\Delta^2 R_1 I_e + 2m_1m_0 R_1 \left(1 - \frac{\Sigma_{1+}}{\delta_1} + \frac{(\delta_1 + m_1^2)(\delta_1 + \Sigma_{1-})}{\Delta\delta_1} \right) I_e \right. \\
 &+ R_1 \left(\Sigma_{1-} - 3\Sigma_{1-} - \frac{2}{\delta_1} (\Delta^2 + 2m_1^2\Sigma_{1-}) - \frac{(\delta_1 - \Sigma_{1-})(\delta_1 + \Sigma_{1+})}{2(\delta_1 + m_1^2)} \right. \\
 &+ \frac{\delta_1 + m_1^2}{\Delta\delta_1} [-\delta_1^2 + 4(m_1^2\Sigma_{1-} - \Delta^2) - 3\delta_1\Sigma_{1-}] \left. \right) I_e \left. \right\}
 \end{aligned}$$

with

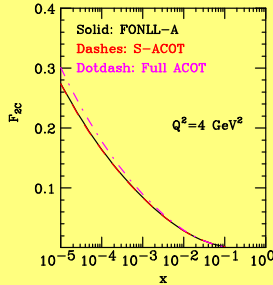
$$I_e \equiv \ln \left(\frac{\Sigma_{1+} + \delta_1 - \Delta}{\Sigma_{1+} + \delta_1 + \Delta} \right)$$

and

$$I_e = \left(\frac{\delta_1 + 2m_1^2}{\delta_1} + \frac{\delta_1 + m_1^2}{\Delta\delta_1} \Sigma_{1+} \right) I_e.$$

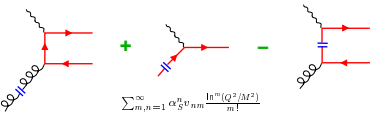
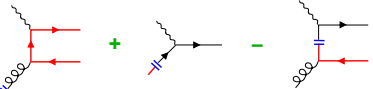
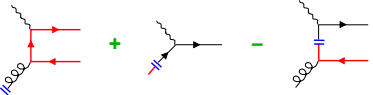
S-ACOT

$$\begin{aligned}
 C_2^{(V,0)} &= C_2(F) \frac{x}{2} \left[\frac{1+x^2}{1-x} \left(\ln \frac{(1-x)}{x} - \frac{3}{4} \right) + \frac{1}{4}(9+5x) \right]_+, \\
 C_1^{(V,0)} &= \frac{1}{2x} C_2^{(V,0)} - C_2(F) \frac{1}{2} x, \\
 C_3^{(V,0)} &= \frac{1}{x} C_2^{(V,0)} - C_2(F)(1+x),
 \end{aligned}$$



J. Rojo et al., arXiv:1003.1241

Three versions of the ACOT scheme

Scheme	Lowest-order graphs	Variables in H_c
Full ACOT <i>Aivasis et. al., hep-ph/9312319</i> <i>Proof in Collins, hep-ph/9806259</i>	 $\sum_{m,n=1}^{\infty} \alpha_s^n v_{nm} \frac{\ln^m(Q^2/M^2)}{m!}$	$m_c \neq 0$ $\zeta = \frac{\beta}{2} \left(1 + \sqrt{1 + \frac{4m_c^2}{Q^2}} \right)$
Simplified ACOT <i>Proof in Collins, hep-ph/9806259;</i> <i>Kramer, Olness, Soper, hep-ph/0003035</i>		$m_c = 0$ $\zeta = x$
S-ACOT-χ <i>Tung, Kretzer, Schmidt, hep-ph/0110247;</i> <i>proof in Guzzi et al., arXiv:1108.5112</i>		$m_c = 0$ $\zeta = x \left(1 + \frac{4m_c^2}{Q^2} \right) \equiv \chi$

■ H_a with incoming light partons are unambiguous

■ H_c with incoming c quarks differ by terms of order $(m_c^2/Q^2)^p, p > 0$

Energy conservation near the threshold

Threshold rate suppression resulting from energy conservation is the most important mass effect at $Q \approx m_c$

(Tung, Kretzer, Schmidt, hep-ph/0110247; Tung, Thorne, arXiv:0809.0714; P.N., Tung, arXiv:0903.2667)

In DIS, a $c\bar{c}$ pair is produced only at partonic energies \widehat{W} satisfying

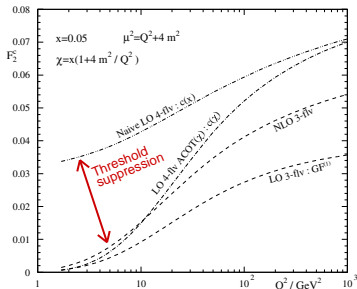
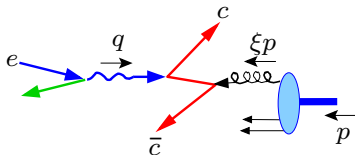
$$\widehat{W}^2 = (\xi p + q)^2 = Q^2 \left(\frac{\xi}{x} - 1 \right) \geq 4m_c^2$$

$$\Rightarrow \chi \leq \xi \leq 1, \text{ where } \chi \equiv x \left(1 + \frac{4m_c^2}{Q^2} \right) \geq x.$$

☹ Collinear approximation for $c\bar{c}$ production may allow to integrate over

$$x \leq \xi \leq 1,$$

in violation of energy conservation



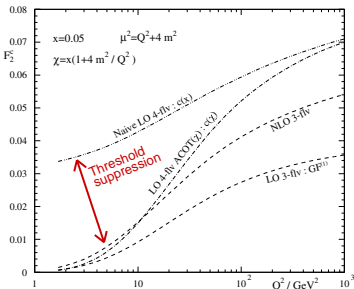
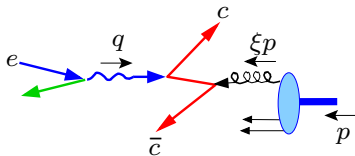
Energy conservation near the threshold

Threshold rate suppression resulting from energy conservation is the most important mass effect at $Q \approx m_c$

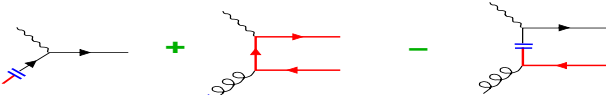
(Tung, Kretzer, Schmidt, hep-ph/0110247; Tung, Thorne, arXiv:0809.0714; P.N., Tung, arXiv:0903.2667)

☺ The S-ACOT- χ scheme allows one to include the energy conservation requirement in the **QCD factorization theorem** (arXiv:1108.5112)

☺ This is achieved by **rescaling** (Barnett, 1976; Tung et al., 2002), which restores the correct kinematics of HQ production without *a posteriori* constraints or damping factors imposed by other schemes



Rescaling at the lowest order



$$c(\zeta) + \frac{\alpha_s}{4\pi} \int_{\chi}^1 \frac{d\xi}{\xi} g(\xi) C_{h,g}^{(1)}\left(\frac{\chi}{\xi}\right) - \frac{\alpha_s}{4\pi} \int_{\zeta}^1 \frac{d\xi}{\xi} g(\xi) A_{h,g}^{(1)}\left(\frac{\zeta}{\xi}\right)$$

ζ takes place of x
in terms 1 and 3

- Term 2 (γ^*g fusion) is unambiguous
- Terms 1 and 3 are essentially

$$\int_0^1 \frac{d\xi}{\xi} \delta\left(1 - \frac{\zeta}{\xi}\right) c(\xi) - \frac{\alpha_s}{4\pi} \int_0^1 \frac{d\xi}{\xi} g(\xi) A_{h,g}^{(1)}\left(\frac{\zeta}{\xi}\right) \theta\left(1 - \frac{\zeta}{\xi}\right).$$

Rescaling $\zeta \rightarrow \kappa\zeta$, $\xi \rightarrow \kappa^{-1}\xi$ changes the ξ range in the **Wilson** coefficients $\delta\left(1 - \frac{\zeta}{\xi}\right)$ and $A_{h,g}^{(1)}\left(\frac{\zeta}{\xi}\right) \theta\left(1 - \frac{\zeta}{\xi}\right)$, but does not change their magnitude

Rescaling at the lowest order

$$c(\zeta) + \frac{\alpha_s}{4\pi} \int_{\chi}^1 \frac{d\xi}{\xi} g(\xi) C_{h,g}^{(1)}\left(\frac{\chi}{\xi}\right) - \frac{\alpha_s}{4\pi} \int_{\zeta}^1 \frac{d\xi}{\xi} g(\xi) A_{h,g}^{(1)}\left(\frac{\zeta}{\xi}\right)$$

ζ takes place of x
in terms 1 and 3

$$Q^2 = 10 \text{ GeV}^2$$

■ **Red curve:** $g(\xi)C_{h,g}^{(1)}(\chi/\xi)$ at $\chi \leq \xi \leq 1$

■ **Green:** $\zeta = \mathbf{x}; \kappa = 1$

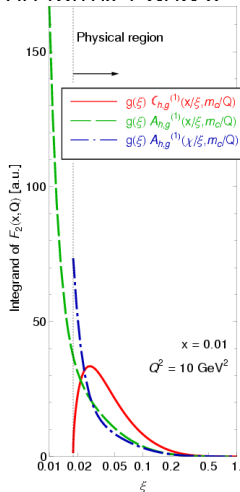
▶ $g(\xi)A_{h,g}^{(1)}(x/\xi) \neq 0$ at $\xi < \chi$

▶ its integral cancels poorly with $c(x)$

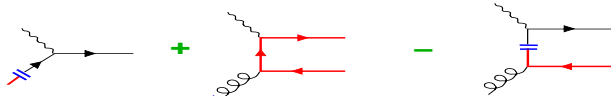
■ **Blue:** $\zeta = \chi; \kappa = 1 + 4m_c^2/Q^2$

▶ $g(\xi)A_{h,g}^{(1)}(\chi/\xi) = 0$ at $\xi < \chi$

▶ its integral cancels better with $c(\chi)$



Rescaling at the lowest order



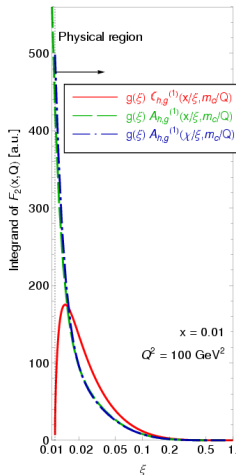
$$c(\zeta) + \frac{\alpha_s}{4\pi} \int_{\chi}^1 \frac{d\xi}{\xi} g(\xi) C_{h,g}^{(1)}\left(\frac{\chi}{\xi}\right) - \frac{\alpha_s}{4\pi} \int_{\zeta}^1 \frac{d\xi}{\xi} g(\xi) A_{h,g}^{(1)}\left(\frac{\zeta}{\xi}\right)$$

ζ takes place of x
in terms 1 and 3

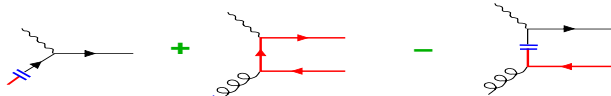
$$Q^2 = 100 \text{ GeV}^2$$

$$\chi \approx x$$

$g(\xi) A_{h,g}^{(1)}(\zeta/\xi)$ approximates the logarithmic growth in $g(\xi) C_{h,g}^{(1)}(\chi/\xi)$

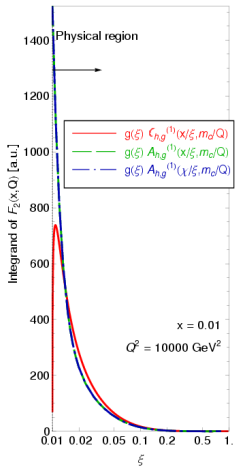


Rescaling at the lowest order



$$c(\zeta) + \frac{\alpha_s}{4\pi} \int_{\chi}^1 \frac{d\xi}{\xi} g(\xi) C_{h,g}^{(1)}\left(\frac{\chi}{\xi}\right) - \frac{\alpha_s}{4\pi} \int_{\zeta}^1 \frac{d\xi}{\xi} g(\xi) A_{h,g}^{(1)}\left(\frac{\zeta}{\xi}\right)$$

ζ takes place of x

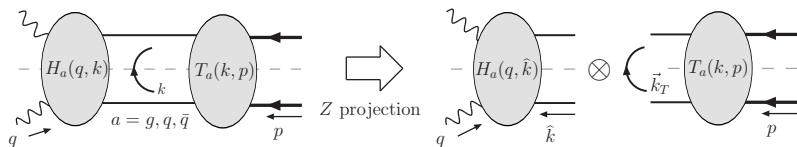


$Q^2 = 10000 \text{ GeV}^2$

$\chi \approx x$

$g(\xi) A_{h,g}^{(1)}(\zeta/\xi)$ approximates the logarithmic growth in $g(\xi) C_{h,g}^{(1)}(\chi/\xi)$

Rescaling to all orders of α_s and the factorization theorem

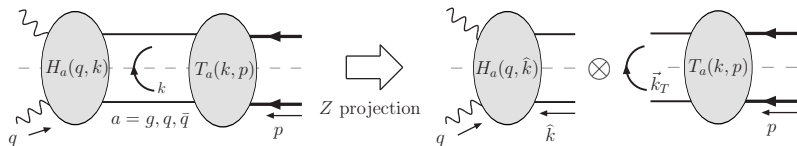


■ Rescaling is introduced in the definition of the hard subgraph $H_c(q, \hat{k})$ with an incoming c quark in $\gamma^*(q) + c(\hat{k}) \rightarrow X$. Hard graphs H_g, H_q with incoming light partons and target graphs $T_a(k, p)$ are not affected

■ In $H_c(q, \hat{k})$, the momentum of the incoming c quark is approximated by $\hat{k} = (\xi p^+, 0^-, \vec{0}_T) \cdot \hat{k}$ and $H_c(q, \hat{k})$ are invariant under transformation $p^+ \rightarrow p^+/\kappa, \xi \rightarrow \xi \kappa$. The physical ξ range is obtained for $\kappa = 1 + 4m_c^2/Q^2$.

■ This transformation shows that the S-ACOT- χ scheme is valid to all orders on the same grounds as the S-ACOT scheme.

Rescaling to all orders of α_s and the factorization theorem



$$F(x, Q) = \sum_{a=g,u,d,\dots,c} \int \frac{d\xi}{\xi} C_a \left(\frac{x}{\xi}, \frac{Q}{\mu}, \frac{m_c}{Q} \right) f_{a/p}(\xi, \mu)$$

■ Wilson coefficients with initial heavy quarks are

$$C_c \left(\frac{x}{\xi}, \frac{Q}{\mu}, \frac{m_c}{Q} \right) \approx C_c \left(\frac{\chi}{\xi}, \frac{Q}{\mu}, m_c = 0 \right) \theta(\chi \leq \xi \leq 1)$$

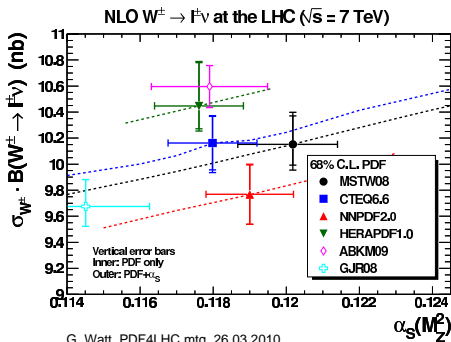
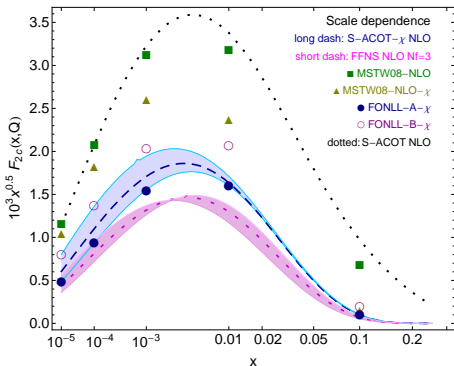
$$\text{where } \chi \equiv x \left(1 + \frac{4m_c^2}{Q^2} \right).$$

■ The target (PDF) subgraphs T_a are given by the same **universal** operator matrix elements in all ACOT schemes

Heavy-quark NC DIS at NLO

At NLO, the charm mass m_c and factorization scale μ of are **tuned** to best describe the DIS data in each scheme; but the residual differences in the W and Z cross sections remain

LH PDFs $Q=2$ GeV, $m_c=1.41$ GeV

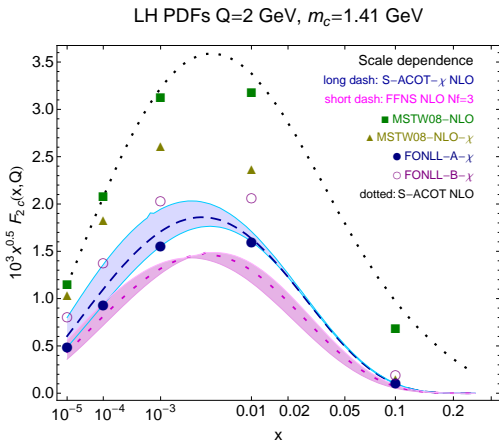


2009 Les Houches HQ benchmarks
 with toy PDFs; default $\mu = Q$

W, Z cross sections;
 $m_c = 1.3$ GeV in CTEQ6.6

NNLO results for $F_2^{(c)}(x, Q^2)$

At NLO:



NNLO results for $F_2^{(c)}(x, Q^2)$

At NNLO and $Q \approx m_c$:

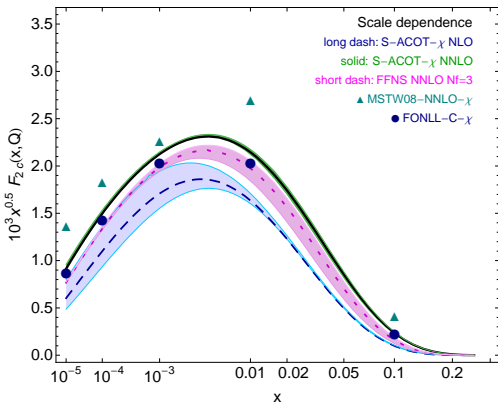
S-ACOT- χ ($N_f = 4$) \approx FFN ($N_f = 3$)
without tuning

■ S-ACOT is numerically close to other NNLO schemes

■ NNLO expressions are close to the FONLL-C scheme

(Forte, Laenen, Nason, *arXiv:1001.2312*).

LH PDFs $Q=2$ GeV, $m_c=1.41$ GeV



NNLO results for $F_2^{(c)}(x, Q^2)$

At NNLO and $Q \approx m_c$:

S-ACOT- $\chi(N_f = 4) \approx$ FFN($N_f = 3$)
without tuning

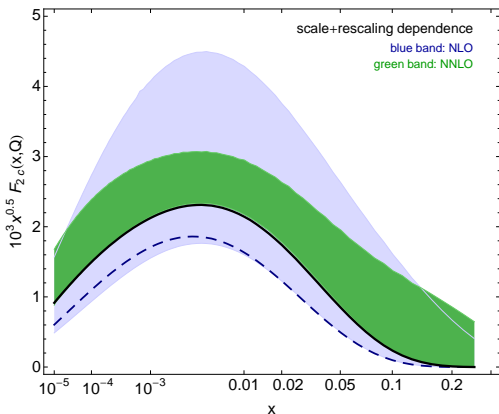
■ S-ACOT is numerically close to other NNLO schemes

■ NNLO expressions are close to the FONLL-C scheme

(Forte, Laenen, Nason, *arXiv:1001.2312*).

■ Even without rescaling (**a wrong choice!**), NNLO cross sections are much closer to FFN at $Q \approx m_c$ than at NLO

LH PDFs $Q=2$ GeV S-ACOT



Main features of the S-ACOT- χ scheme

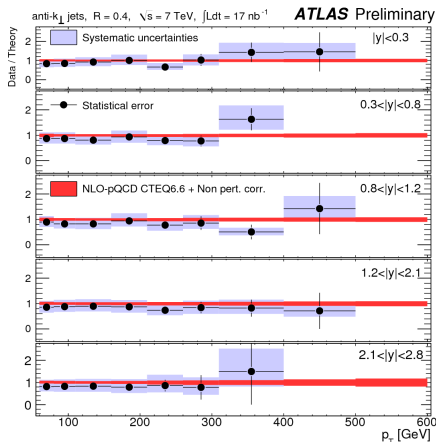
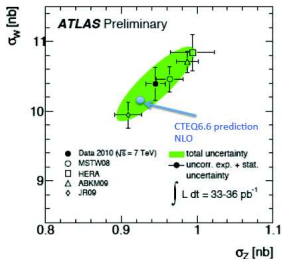
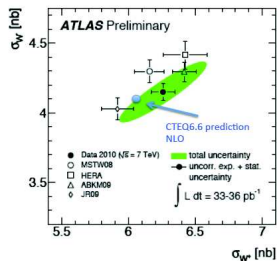
- It is proved to all orders by the QCD factorization theorem for DIS (*Collins, 1998*)
- It is relatively simple
 - ▶ One value of N_f (and one PDF set) in each Q range
 - ▶ sets $m_h = 0$ in ME with incoming $h = c$ or b
 - ▶ matching to FFN is **implemented as a part of the QCD factorization theorem**
- **Universal** PDFs
- It reduces to the ZM \overline{MS} scheme at $Q^2 \gg m_Q^2$, without additional renormalization
- It reduces to the FFN scheme at $Q^2 \approx m_Q^2$
 - ▶ has reduced dependence on tunable parameters at NNLO

Conclusions

- In the CT10.1 fit, an NNLO calculation for $F_{2,L}^{c,b}$ in the S-ACOT scheme is demonstrated to be viable.
- S-ACOT- χ formalism provides recipe-like formulas for implementing NNLO DIS terms with with heavy quarks
 - ▶ Energy conservation is realized as a part of the QCD factorization theorem by momentum fraction rescaling in Wilson coefficient functions with incoming heavy quarks. The PDFs are given by universal operator matrix elements.
- Progress in understanding of NNLO contributions, new Tevatron and LHC data sets, PDF parametrization issues
- **arXiv:1101.0561**: synopsis of recent CTEQ publications
 - ▶ CT10W fit to Run-2 W charge asymmetry; PDFs for leading-order showering programs; constraints on color-octet fermions

CTEQ PDFs vs. the latest data: LHC

Agreement with many LHC measurements



+data on σ_W/σ_Z , $t\bar{t}$, $\gamma\gamma$, etc.

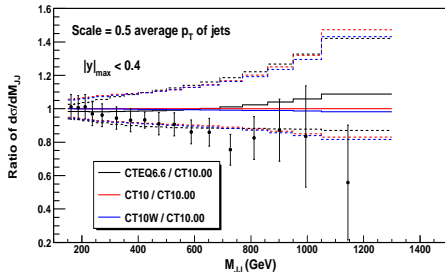
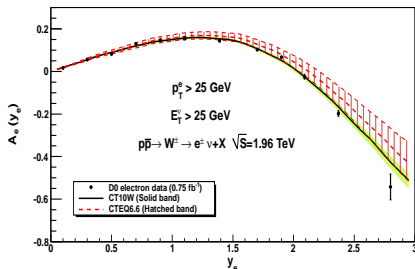
Figures are from ATLAS. Similar results from CMS

CTEQ PDFs vs. the latest data: Tevatron

Outstanding puzzles:

1. Run-2 W charge asymmetry (constraining $d(x, Q)/u(x, Q)$ at $x > 0.1$)
2. Inclusive (di)jet production (constraining $g(x, Q)$ at $x > 0.1$)

In both processes, experimental accuracy is high enough to start feeling effects beyond NLO and of resummations



The puzzle of the CDF/D0 W lepton asymmetry

- CT10W set reasonably agrees with 3 $p_{T\ell}$ bins of $A_e(y_e)$ and one bin of $A_\mu(y_\mu)$ from D0 Run-2 (2008).
- NNPDF 2.0 (*arXiv:1012.0836*) agrees with $A_\mu(y_\mu)$, disagrees with two $p_{T\ell}$ bins of $A_e(y_e)$.
- CT10, many other PDFs fail.

Agreement of PQCD with D0 $A_e(y_e)$	χ^2/n_{pt}	Source or comments
CTEQ6.6, NLO	191/36=5.5	<i>Our study;</i> <i>Resbos, NNLL-NLO</i>
CT10W, NLO	78/36=2.2 With $A_\mu(y_\mu)$: 88/47=1.9	
ABKM'09, NNLO	540/24=22.5	<i>Catani, Ferrera, Grazzini,</i> <i>JHEP 05, 006 (2010)</i>
MSTW'08, NNLO	205/24=8.6	
JR09VF, NNLO	113/24=4.7	

Why difficulties with fitting $A_\ell(y_\ell)$?

1. $A_\ell(y_\ell)$ is very sensitive to the average slope s_{du} of $d(x, M_W)/u(x, M_W)$

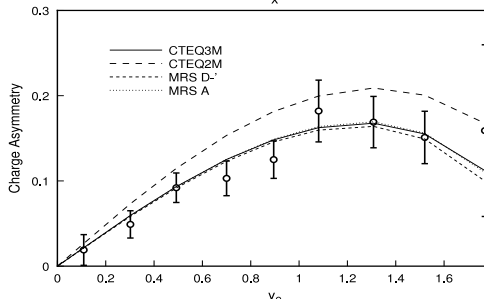
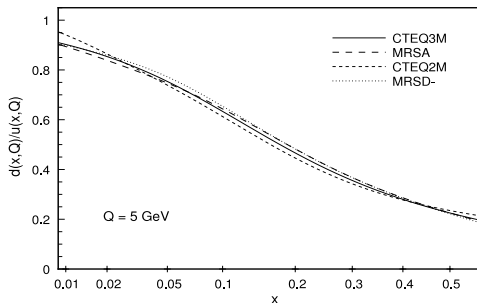
$$A_\ell(y_\ell) \sim A_\ell(y_W)|_{LO} \propto \frac{1}{x_1 - x_2} \left[\frac{d(x_1)}{u(x_1)} - \frac{d(x_2)}{u(x_2)} \right]; \quad x_{1,2} = \frac{Q}{\sqrt{s}} e^{\pm y_W}$$

Berger, Halzen, Kim, Willenbrock, PRD 40, 83 (1989); Martin, Stirling, Roberts, MPLA 4, 1135 (1989); PRD D50, 6734 (1994); Lai et al., PRD 51, 4763 (1995)

2. Constraints on s_{du} by fixed-target $F_2^d(x, Q)/F_2^p(x, Q)$ are affected by nuclear and higher-twist effects

Accardi, Christy, Keppel, Monaghan, Melnitchouk, Morfin, Owens, PRD 81, 034016 (2010)

Challenges with fitting $A_\ell(y_\ell)$



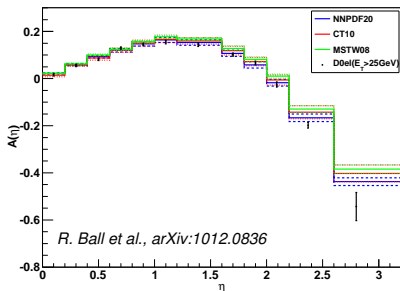
Small changes in s_{du} cause significant variations in A_ℓ

Lai et al., PRD 51, 4763 (1995)

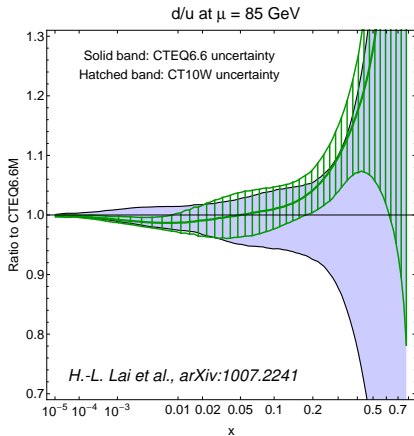
Alternative constraints on d/u by $F_2^d(x, Q)/F_2^p(x, Q)$ from fixed-target DIS are affected by nuclear and higher-twist effects

Accardi, Christy, Keppel, Monaghan, Melnitchouk, Morfin, Owens, PRD 81, 034016 (2010)

$d(x, Q)/u(x, Q)$ at $Q = 85$ GeV



R. Ball et al., arXiv:1012.0836



H.-L. Lai et al., arXiv:1007.2241

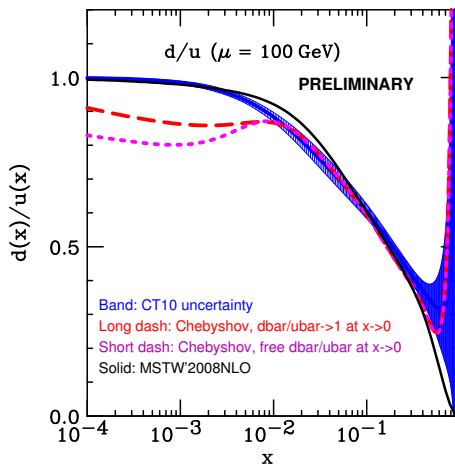
■ D0 Run-2 A_ℓ data distinguishes between PDF models, reduces the PDF uncertainty

Why difficulties with fitting $A_\ell(y_\ell)$?

3. Existing parametrizations underestimate the PDF uncertainty on d/u

PDFs based on Chebyshev polynomials improve agreement with D0 Run-2 A_e , but are outside of current CTEQ/MSTW bands (*Pumpplin*)

This ambiguity is reduced by $A_\ell(y_\ell)$ at the LHC, which constrains d/u and \bar{d}/\bar{u} at $x \sim 0.01$.



Why difficulties with fitting $A_\ell(y_\ell)$?

4. Experimental A_ℓ with lepton $p_{T\ell}$ cuts is sensitive to $d\sigma/dq_T$ of W boson at transverse momentum $q_T \rightarrow 0$.

- Fixed-order (N)NLO calculations (DYNNLO, FEWZ, MCFM,...) predict a wrong shape of $d\sigma/dq_T$ at $q_T \rightarrow 0$.
- Small- q_T resummation correctly predicts $d\sigma/dq_T$ in this limit.
- CT10(W) PDFs are fitted using a NNLL-NLO+K resummed prediction for A_ℓ (ResBos); **must not be used with fixed-order predictions for A_ℓ .**

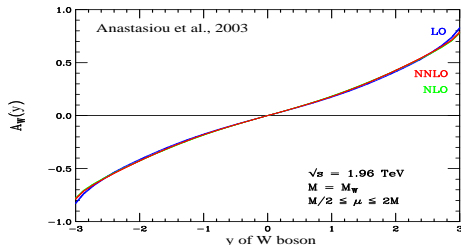
For example:

$$\chi^2(\text{CT10W+ResBos}) = 1.9 N_{pt} \text{ (us);}$$

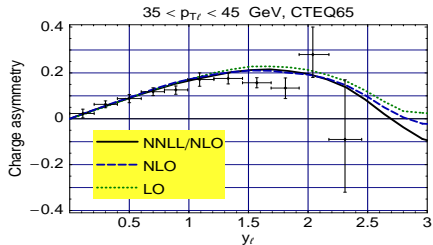
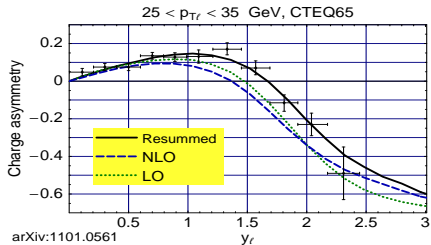
$$\chi^2(\text{CT10W+DYNNLO}) = 8.4 N_{pt} \text{ (NNPDF)}$$

Charge asymmetry in p_T^e bins (CDF Run-2, 207 pb⁻¹)

Without the p_T^e cut (FEWZ):

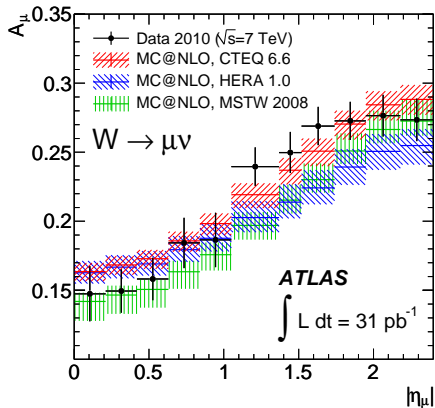


With p_{T_e} cuts imposed, $A_{ch}(y_e)$ is sensitive to small- Q_T resummation

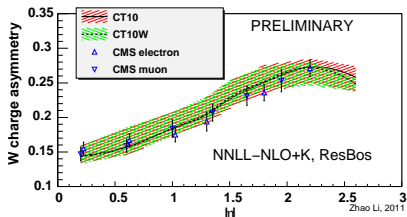
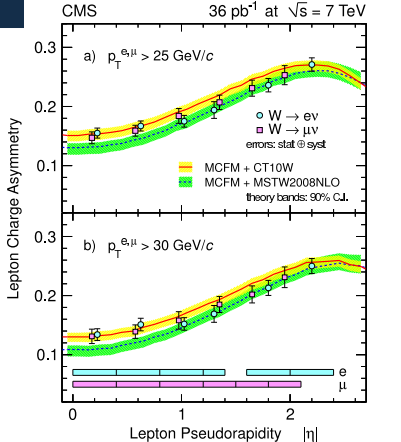


PN, 2007, unpublished; arXiv:1101.0561

CT10(W) vs. A_ℓ at the LHC

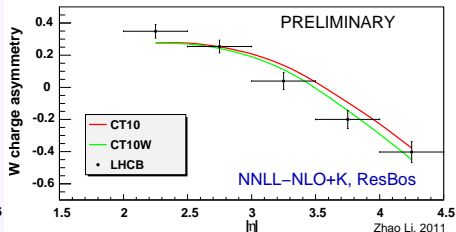
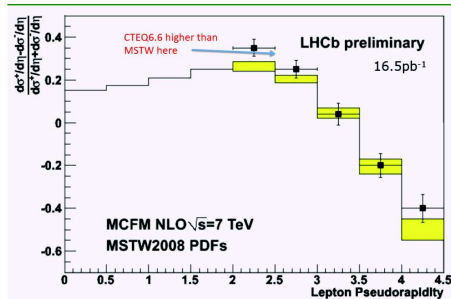


CT10(W) agrees well with the LHC A_ℓ ; some differences between NLO and NNLL+NLO



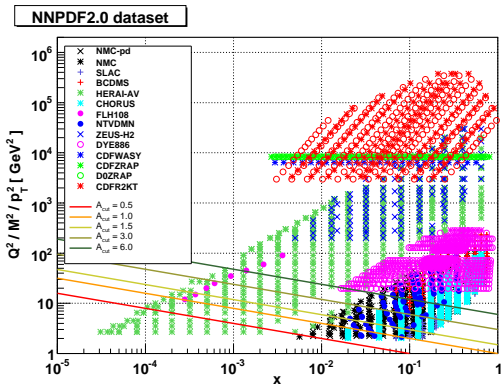
CT10(W) vs. A_ℓ : LHC-B

LHCb asymmetry measurement; from PDF4LHC Mar 7



LHC-B marginally prefers CT10W

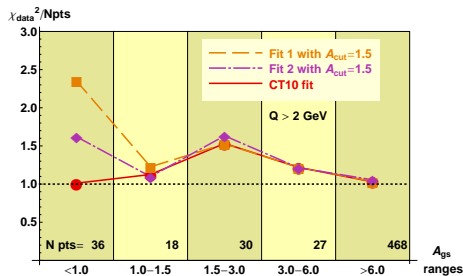
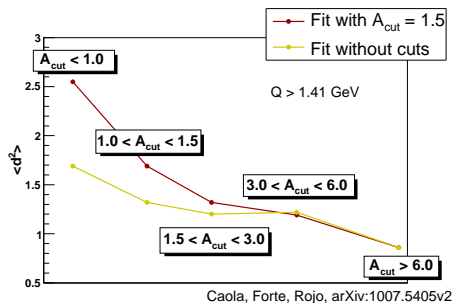
A_{cut} fits to combined HERA data



Fitting procedure:

- Include only DIS data above an A_{cut} line
- Compare the resulting PDFs with DIS data below the A_{cut} line, in a region that is “connected” by DGLAP evolution

CT10: A_{cut} fits to DIS data at $Q > Q_0 = 2 \text{ GeV}$

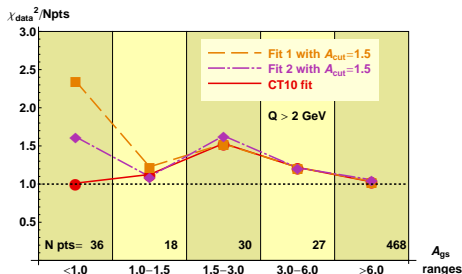
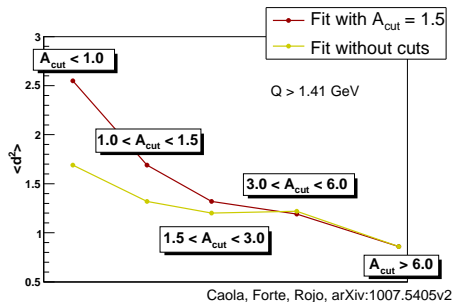


Motivation

Search for deviations from DGLAP evolution at smallest x and Q

■ Follow the procedure proposed by NNPDF (Caola, Forte, Rojo, arXiv:1007.5405)

CT10: A_{cut} fits to DIS data at $Q > Q_0 = 2 \text{ GeV}$



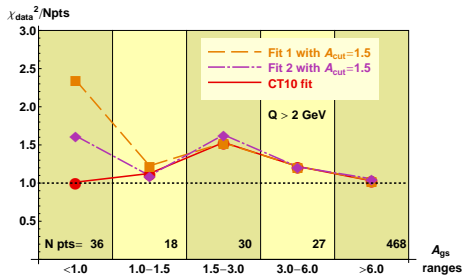
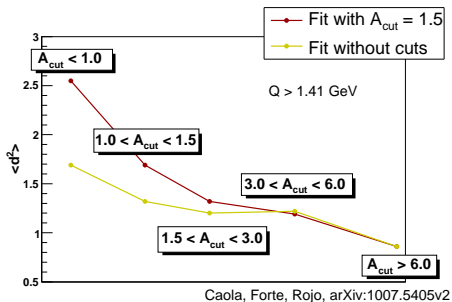
CT10

Two CT10-like fits to data at $A_{gs} > 1.5$, with different parametrizations of $g(x, Q)$

$$\chi_i^2 = \frac{(\text{Shifted Data} - \text{Theory})^2}{\sigma_{uncor}^2}$$

Large syst. shifts at $A_{gs} < 1.0$, in a pattern that could mimic a slower Q^2 evolution

CT10: A_{cut} fits to DIS data at $Q > Q_0 = 2 \text{ GeV}$



CT10, cont.

$\delta\chi^2 \sim 0$ at $A_{gs} > 1.0$
(no difference)

$\delta\chi^2 = 0 - 1.5$ at $A_{gs} < 1.0$,
with large uncertainty

\Rightarrow Disagreement with the "DGLAP-connected" data at $A_{gs} < A_{cut}$ is not supported by the CT10 fit

$\chi^2/N_{data\ points}$ in various experiments (PRELIMINARY)

PDF set	Order	All expts.	Combined HERA-1 DIS	BCDMS $F_2^{p,d}$	CDF, D0 Run-2 1-jet	D0 Run-2 A_{ch}^e , $p_T^e > 25\ GeV$
CT10.1	NLO	1.11	1.17	1.10	1.33	3.72
MSTW08		1.42 (1.28)	1.73 (1.4)	1.16 (1.17)	1.31	11.38
NNPDF2.0		1.37	1.32	1.28	1.57	2.79
CT10.1	NNLO	1.13	1.12	1.14	1.23	2.59
MSTW08		1.34	1.36	1.15	1.38	9.84
NNPDF2.1		1.57	1.36	1.30	1.51	5.45
ABM'09 (5f)		1.65	1.4	1.49	2.63	23.78
HERA1.5		1.71	1.15	1.87	?	5.4

N_{points}

2798

579

590

182

12

Cross sections are computed using the CTEQ fitting code and α_s , m_c , m_b values provided by each PDF set. Their agreement does not immediately improve after going to NNLO.

Comparison of (N)NLO PDF sets with data in the CT10.1 fit

- χ^2 are computed at NNLO, using the LHAPDF 5.8.6 interface and **CTEQ fitting code (very naively!)**
- Whenever possible, adjust settings to reproduce assumptions by other groups
 - ▶ Use $\alpha_s(M_z)$, $m_{c,b}$ values suggested by each PDF set
 - ▶ approximate the GM scheme in DIS if possible
- Correlated systematic errors are included according to the CTEQ method

$$\chi^2 = \sum_{e=\{\text{expt.}\}} \left[\sum_{k=1}^{N_{pt}} \frac{1}{s_k^2} \left(D_k - T_k - \sum_{\alpha=1}^{N_\lambda} \lambda_\alpha \beta_{k\alpha} \right)^2 + \sum_{\alpha=1}^{N_\lambda} \lambda_\alpha^2 \right]$$

- ▲ D_k and T_k are data and theory values ($k = 1, \dots, N_{pt}$);
- ▲ s_k is the stat.+syst. uncorrelated error; λ_α are sources of syst. errors